IEEE Access
Multidisciplinary ⋮ Rapid Review ⋮ Open Access Journal

Received 30 September 2023, accepted 9 October 2023, date of publication 11 October 2023, date of current version 17 October 2023.

Digital Object Identifier 10.1109/ACCESS.2023.3323951

RESEARCH ARTICLE

Research on Collaborative Task Allocation of Heterogeneous UAVs With Complex Constraints

SHAOKUN YAN[1,2] AND YUANQING XIA[1], (Senior Member, IEEE)
[1]School of Automation, Beijing Institute of Technology, Beijing 100081, China
[2]Jiangsu Automation Research Institute, Lianyungang 222000, China

Corresponding author: Shaokun Yan (yanshaokun@foxmail.com)

ABSTRACT This paper addresses the multi-task allocation problem with complex constraints in the multi-UAV system by presenting an extension to consensus-based bundle algorithm(CBBA). The presented algorithm termed dynamic clustering consensus-based bundle algorithm(DCCBBA) provides an improved bundle construction, a novel consensus strategy and a systematic way of grouping. DCCBBA features different consensus methods for inner conflict resolution and outer conflict resolution. The inner conflict resolution aims at handling the violated task assignment that belongs to the same cluster, while outer conflict resolution guarantees conflict-free assignments in the overall UAVs. The proposed DCCBBA coupled with Pythagorean Hodograph curves can significantly reduce the number of communication events required to achieve consensus while preserving the robust convergence property of the baseline CBBA. Numerical simulations on various cooperative reconnaissance and strike tasks demonstrate the reduction of communication events compared with the baseline CBBA, the cluster-formed CBBA, the grouped CBBA and Two-layer CBBA.

INDEX TERMS CBBA, communication network topology, heterogeneous UAVs, task allocation.

I. INTRODUCTION

Multi-UAV system has been increasingly drawing a wide interest over a single UAV as it is more capable of accomplishing difficult and complex missions in both civil and military arenas, such as surveillance and reconnaissance, search and rescue, smart agriculture and disaster response [1] in an effective and efficient manner and it is more fault tolerant [2]. Multi-UAV task allocation has become a prominent area of investigation. In a task allocation problem, a group of UAVs services a finite number of tasks to optimize an overall system objective required by the mission. In practical application, task allocation problem is becoming increasingly complex due to the heterogeneity of UAVs, the complexity of tasks, the limitations on communication and the robustness of allocation algorithms [3], [4]. Besides, the multi-UAV task allocation has been shown to be NP-hard and a variety of approximate methods [5], [6] have been developed to efficiently produce solutions to the assignment problem.

Depending on who solves the assignment problem, solutions to task assignment problems fall under two broad categories: centralized or decentralized. Centralized methods involve all the UAVs sending relevant data to the central control station which produces task assignments for all the UAVs, the central control station sends out allocation results to individual UAVs. Centralized methods fit easily into the human centered model, where an operator manages the team of UAVs. However, centralized methods suffer from several weaknesses especially for complex situations. First, consistent communication is required to produce conflict-free assignments, which places a heavy communication burden on the communication network. Second, the computational demand is high as the computational operations are all placed on the central control station, it may result in latency in making allocation decisions. Third, if the central control station is damaged, the whole task assignment structure in the multi-UAV system will be destroyed. Centralized methods are vulnerable to the single point of failure. In contrast, each

The associate editor coordinating the review of this manuscript and approving it for publication was Guillermo Valencia-Palomo.

UAV in the decentralized methods independently produces a task assignment solution based on its own perceived information, and then obtains the global solution for the multi-UAV system through communication and negotiation. Thus, decentralized task assignment methods have great robustness and fault tolerance, which is suitable for solving the cooperative multi-UAV task assignment problem with complex constraints. The consensus based bundle algorithm (CBBA) [7], which leads each agent to agree upon the plan via a sequence of local communication, is a decentralized method to resolve multi-agent task assignment problems. CBBA consists of two phases: the bundle construction phase that utilizes the sequential greedy algorithm (SGA) to build task sequence, and the conflict resolution phase that uses the consensus strategy to achieve global agreement.

At present, numerous versions of CBBA have been proposed from different perspectives. Decentralized methods for allocating heterogeneous tasks to a network of agents with different capabilities are presented in [8], which increases the cooperation constraints of robots and proposes a new scoring mechanism. A new auction and consensus based algorithm for fast task allocation in parallel with task execution is proposed. Each robot only bids for the task with the highest score in the auction phase to produce conflict-free assignments in [9]. Combining the CBBA with the ant colony system, the bundle construction phase utilizes ant colony optimization, but the algorithm has a higher complexity and a longer running time in [10]. Asynchronous Consensus Based Bundle Algorithm(ACBBA) extends CBBA to maximize the flexibility in a distributed environment, it breaks the synchronous assumptions of the CBBA while preserving the convergence properties in [11] and [12]. A CBBA-based method is used to solve the task assignment problem of multi-UAV material delivery, and a ''closed-loop CBBA'' that considers returning to the take-off base after the completion of tasks is proposed in [13]. Inspired by CBBA, a Performance Impact (PI) algorithm is proposed, the key point to the algorithm is to define a concept of significance, which is used to measure the contribution of the task assigned to the robot to the local cost of the robot in [14]. The above CBBA algorithm and its extensions can only achieve convergence within a limited time and obtain conflict-free task assignments when UAVs are in fully connected networks.

Equally, communication constraints play an important role in determining the capabilities of task assignments in CBBA. As the number of UAVs or tasks in the network increases, it inevitably leads to substantial communication costs and may overflow the network bandwidth. To address this issue, several extensions of the CBBA [15], [16], [17], [18], [19], [20] have presented ways to reduce the communication loads in the consensus process. Communication of the system will be reduced if only a part of the UAVs is involved in the communication. Based on the above ideas, many scholars carry out task allocation work from the perspective of clustering. Team CBBA (T-CBBA) [15] gives a manageable architecture for large numbers of unmanned agents through human centered operations if teams are divided in advance, which encourages cooperation between groups of agents on complex tasks. The cluster-formed CBBA(CF-CBBA) [16] is designed to reduce the amount of communication required to reach a conflict-free assignment by partitioning the problem and processing in parallel. A cluster-first strategy [17] which builds upon existing consensus-based distributed task allocation algorithms is proposed to solve task allocation problems in search and rescue scenarios. The key point is that assigning a group of tasks that are clustered to a robot is more likely to result in an efficient schedule. A two-layer task assignment algorithm based on feature weight clustering is presented in [18], the UAV swarm and tasks are divided into multiple clusters to get a conflict-free task assignment solution in real time. The grouped CBBA(GCBBA) [20] provides a systematic way of grouping the UAVs based on their task preference represented by the initial bundle construction, which can improve the communication efficiency by reducing the requirments for propagating irrelevant bids while preserving the framework of CBBA. In addition, references [12], [21], [22], [23], [24] provide a variety of alternative CBBA improvement algorithms to solve the tasks assignment problem.

II. DISCUSSION ON RELATED WORKS

CBBA using cluster algorithm has been shown, in comparison with baseline CBBA,to require less communication and preserve the robust convergence property when allocating tasks. There are methodologies mentioned above [15], [17], [18], [20], but in most cases, the number of clusters is specified in advance or always remains unchanged, which may be affected by subjective factors and obtain locally optimal solutions. Moreover, although the aforementioned versions of CBBA have made some improvements to reduce the communication loads, the computational complexity of task allocation with complex constraints, such as time window, task allocation with duo cooperation and heterogeneous UAVs is still a crucial problem. Finally, most task allocation algorithms separate the task allocation from path planning. Conflict-free assignments are produced in a weak coupling manner, which results in a great difference between the UAV voyage calculated by the task allocation and the actual voyage. This paper presents a dynamic clustering consensus-based bundle algorithm(DCCBBA), which extends baseline CBBA with an improved bundle construction, a different consensus strategy and a new grouping policy to further reduce the communication between UAVs so that conflict-free assignments can be produced in time.

The main contributions of this paper are two-fold: (i) bundle construction is improved, and different consensus methods for inner conflict resolution and outer conflict resolution are presented to resolve the multi-UAV collaborative task allocation problem with complex constraints while preserving the robust convergence property of the baseline CBBA. Numerical simulations have been performed to

illustrate the performance of DCCBBA under different scales of tasks, different communication topologies and different communication network density. (ii) The proposed DCCBBA strongly couples task allocation with path planning, fifth order Pythagorean Hodograph curves are used in the task allocation to obtain UAV paths, which are closer to flyable paths.

III. TASK ALLOCATION PROBLEM

The upmost objective of heterogeneous task allocation is certainly, given a list of N_T tasks with complex constraints and a list of N_a UAVs of different types, to complete all the mission requirements and it is desirable to maximize or minimize some goal reward in an as efficient as possible manner. The key symbols used hereafter are listed in TABLE 1. In addition, UAVs can exhibit different capabilities and capacities. Different constraints such as, time windows, types or urgency are considered as well in the task allocation. Multiple-UAV task allocation problem and the key procedure of baseline CBBA are briefly described in the section.

A. PROBLEM STATEMENT

The paper focus on the decentralized cooperative multi-UAV task assignment in the reconnaissance and strike scenarios, especially task allocation with duo cooperation and time window constraints. The objective is to obtain a feasible and conflict-free task assignment solution. The allocation problem of heterogenous tasks of the aforementioned category can be expressed as formula (1) and formula (2).

$$\max \sum_{i=1}^{N_a} \sum_{j=1}^{N_T} c_{ij} \cdot x_{ij} \tag{1}$$

subject to

$$\begin{cases} \sum_{j=1}^{N_T} x_{ij} \le L_i \\ \sum_{i=1}^{N_a} x_{ij} \ge num_j \\ \sum_{i=1}^{N_a} \sum_{j=1}^{N_T} x_{ij} \le N_{min} \triangleq \{N_T, N_a \cdot L_i\} \\ t_j \ge t_j^{start} \\ t_j + \Delta t_j \le t_j^{end} \\ d_i \le D_i^{limit} \end{cases} \tag{2}$$

where N_a, N_T denote the number of UAVs and tasks respectively, $x_i = \{0,1\}^{N_T}$ is the decision vector, $x_{ij} = 1$ represents that task j is assigned to UAV i, c_{ij} represents the reward UAV i would obtain by performing task j, L_i is the maximum number of tasks UAV i can perform, num_j is the number of UAVs required to complete task j, t_j is the time to perform task j, $[t_j^{start}, t_j^{end}]$ is the time window of task j, Δt_j is the time required to complete task j, d_i is the flight distance of UAV i required to complete the assigned tasks, D_i^{limit} is the maximum flight distance of UAV i.

TABLE 1. Symbol definition.

Symbol	Definition
N_a	the number of UAVs
N_T	the number of tasks
c_{ij}	the reward UAV i would obtain by performing task j
L_i	the maximum number of tasks UAV i can perform
num_j	the number of UAVs required to complete task j
t_j	the time to perform task j
$[t_j^{start}, t_j^{end}]$	time window of task j
Δt_j	the time required to complete task j
d_i	the flight distance of UAV i required to complete the assigned tasks
D_i^{limit}	the maximum flight distance of UAV i
b_i	assigned tasks ordered for UAV i
p_i	the order where UAV i performs tasks
y_i	the highest bid for task j based on local situation awareness of UAV i
$z_{ij} = 1$	the UAV i has the highest bid for task j
$S_i^{p_i}$	the total reward for UAV i performing the tasks along p_i
$p_i \oplus_n \{j\}$	the operation that inserts task j right after the nth element of p_i
G	the indicator function that is unity if the argument is true
K_k	the kth initial clustering center
C_x^k, C_y^k	the coordinates of K_k
X_{max}, Y_{max}	the range of map
K	the number of clusters
$D = \{d_1, d_2, \cdots d_{N_a}\}$	sample set of UAV coordinates
$C = \{\mathrm{C}_1, C_2, \cdots C_K\}$	the cluster grouping of UAVs
E	square error of a cluster
μ_k	mean vector of C_k
G_n	communication net
V	the set of nodes in G_n
E	the set of edges in G_n
A	the adjacency matrix of G_n
$BNC(v_i)$	betweenness centrality of UAV i
$CNC(v_i)$	closeness centrality of UAV i
$DC(v_i)$	the degree centrality of UAV i
$EVC(v_i)$	the eigenvector centrality of UAV i
$Y(v_i)$	the importance value of node v_i
Z_i	the winning UAV matrix
Y_i	the winner bid value matrix
b_k	the kth control point
$r(q)$	the path point
$s(q)$	the length of the carve
$\dot{x}, \dot{y}$	the velocity in the x and y directions
v	the flight speed
χ	the heading angle
$\dot{\chi}$	the angular velocity of heading angle
T_b	the total communication events in CBBA
C_b	the number of baseline CBBA rounds
T_d	the total communication events in DCCBBA
C_d	the number of DCCBBA rounds
D_{C_i}	the network diameter of C_i
ρ	the communication network density

B. BASELINE CBBA

This section briefly summarizes the CBBA [7], [25]. CBBA can obtain feasible and conflict-free assignments through iterations between two phases: a bundle building phase and a conflict resolution phase. First, each UAV greedily generates an ordered bundle of tasks based on the local situation awareness in the bundle building phase. Then, each UAV gets the global situation awareness and

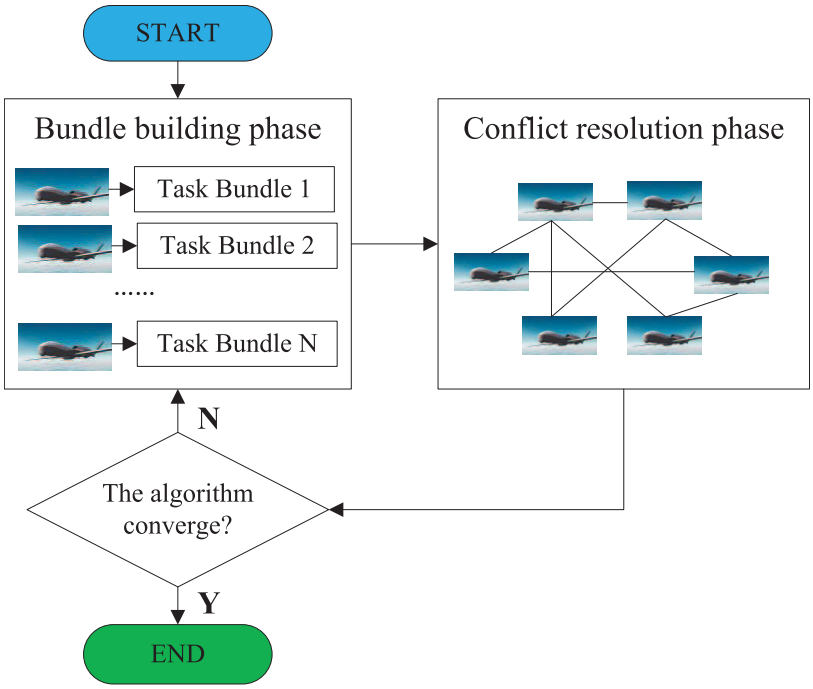

FIGURE 1. Flow diagram of CBBA.

conflicting assignments are identified through mutual communication. These two phases are repeated till convergence. The schematic diagram of CBBA is shown in Fig. 1.

1) BUNDLE CONSTRUCTION PHASE

In the bundle construction phase, UAVs bid on a task and a marginal score is calculated to decide whether a new task should be assigned to the bundle. The bid lists of UAV i can be expressed as follows:

(1) bundle list b_i represents assigned tasks ordered for UAV i based on the greedy task selection.

(2) path list p_i is the order where UAV i performs tasks.

(3) winning bid list y_i represents the highest bid for task j based on local situation awareness of UAV i.

(4) winning UAV list z_i is the corresponding UAV in y_i. $z_{ij} = 1$ represents the UAV i has the highest bid for task j. Otherwise, $z_{ij} = 0$.

In the bundle construction phase, SGA is used to add tasks to b_i and p_i. Then, y_i and z_i are updated according to p_i. The implementation steps of bundle construction are presented in Algorithm 1.

In line 3-5 of algorithm 1, the task that has been selected by the UAV i is eliminated to avoid duplicate tasks in a bundle. In line 7, $S_i^{p_i}$ is the total reward for UAV i performing the tasks along p_i, $p_i \oplus_n \{j\}$ denotes the operation that inserts task j right after the nth element of p_i. In line 8, G is the indicator function that is unity if the argument is true. In line 11, C_j and n_{ij} are intermediate variables.

2) CONFLICT RESOLUTION PHASE

In the conflict resolution phase, the winning bid list y_i and winning UAV list z_i described in the bundle construction phase are communicated for consensus. In addition, s_i which represents the time stamp of the last information is needed to find the latest allocation information. Based on communication with UAV k, there are three possible actions UAV i can take on task j [7].

$$\begin{cases} \text{Update} : y_{ij} = y_{kj}, z_{ij} = z_{kj} \\ \text{Reset} : y_{ij} = 0, z_{ij} = \emptyset \\ \text{Leave} : y_{ij} = y_{ij}, z_{ij} = z_{ij} \end{cases} \tag{3}$$

Algorithm 1 Bundle Construction Phase for UAV i at Iteration t

Input : $b_i(t-1), y_i(t-1), p_i(t-1), z_i(t-1)$
Out : $b_i(t), y_i(t), p_i(t), z_i(t)$
1 : $b_i(t) = b_i(t-1), y_i(t) = y_i(t-1), p_i(t) = p_i(t-1), z_i(t) = z_i(t-1)$
2 : for $j = 1 : N_T$
3 : if $j \in b_i$
4 : $c_{ij} = 0$
5 : $x_{ij} = 0$
6 : else
7 : $c_{ij} = \max_{n \le |p_i|} S_i^{p_i \oplus_n \{j\}} - S_i^{p_i} \quad \forall j \notin b_i$
8 : $x_{ij} = G(c_{ij} > y_{ij})$
9 : end if
10 : while $|b_i(t-1)| < L_i$
11 : $C_j = \arg\max_j (c_{ij} \cdot x_{ij})$
12 : $n_{ij} = \arg\max_n S_i^{p_i \oplus_n \{C_j\}}$
13 : $b_i = b_i \oplus_{end} \{C_j\}, p_i = p_i \oplus_{n_{ij}} \{C_j\}$
14 : $y_{iC_j} = c_{iC_j}, z_{iC_j} = i$
15 : end while
16 : end for

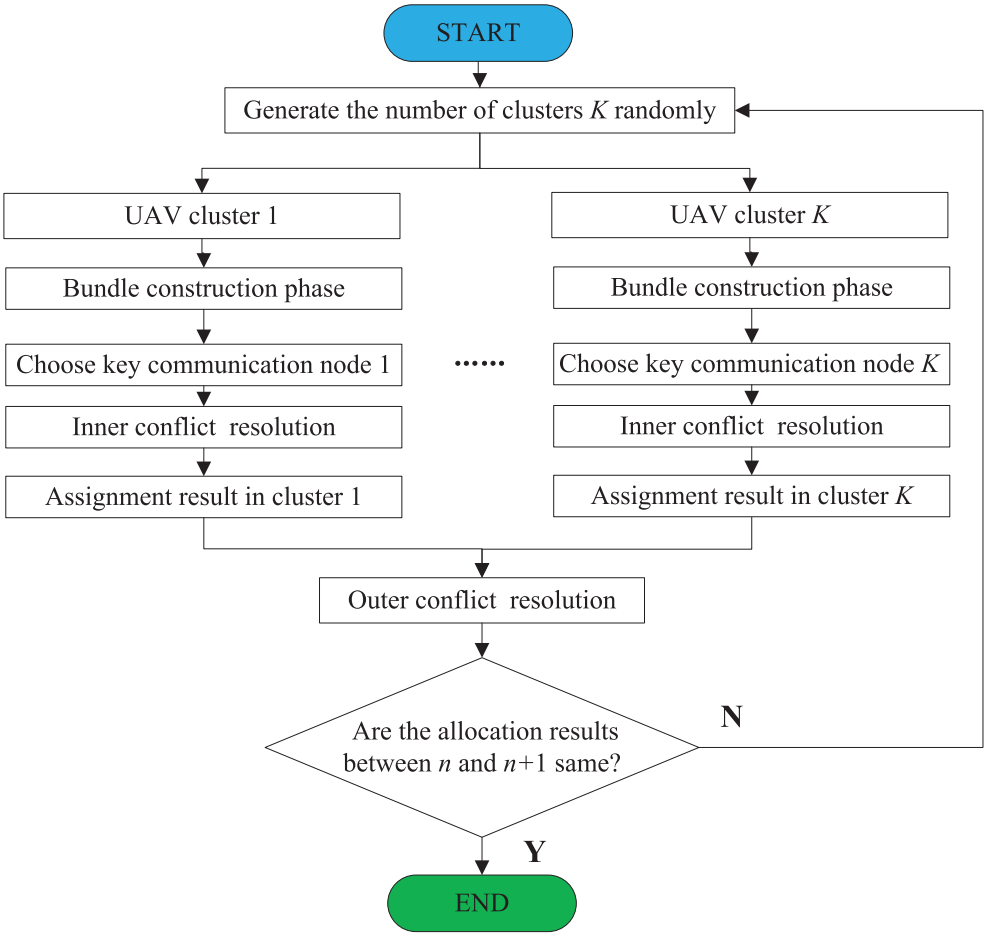

FIGURE 2. The process of DCCBBA.

If a bid is changed as an outcome of communication, each UAV checks whether there are tasks that need to be updated or reset in their bundles, and if so, release them and tasks added after them. Through the conflict resolution phase, y_i and z_i of UAVs will be consensus, and violated tasks can be released from their local bundles.

IV. THE PROPOSED ALGORITHM

The communication required to reach a conflict-free assignment increases exponentially with the increase of AUVs or tasks [8], [14]. If only a part of UAVs participate in the communication, communication between UAVs may be reduced. Inspired by the above idea, the presented DCCBBA coupled with path planning focuses on bringing parallelism to CBBA to reduce the amount of communication, it retains the robustness of distributed task allocation. In addition, the bundle construction phase and conflict resolution phase are redesigned to solve the collaborative task allocation of heterogeneous UAVs with complex constraints. The process of DCCBBA is presented in Fig. 2.

As shown in Fig.2, UAVs are grouped randomly and a vital communication node is selected according to vital communication node model in each cluster. Then, the bundle construction phase and inner-loop consensus phase that consider task allocation with duo cooperation processes in a cluster are presented. Finally, outer-loop construction requires conflict resolution between clusters, which guarantees a conflict-free assignment.

A. GENERATION OF CLUSTERS

Clustering is a fundamental tool in unsupervised learning, used to group objects by distinguishing between similar and dissimilar features of a given data set [26]. The main objective using cluster analysis is to reduce useless communication, and preserve the robust convergence performance. Repeated shuttling in the battlefield greatly increases the danger and exposure probability. Thus, it is natural that a closer task has a more reward to an UAV and the K-means algorithm is used to generation of UAV clusters.

The K-means algorithm requires a predetermined clustering center, some UAVs are randomly selecting as initial clustering centers. However, uncertain initial clustering centers may result in inconsistent grouping and it is necessary to set determined initial clustering centers. Instead of randomly selecting initial values for all cluster centers as is the case with most global clustering algorithms, a new cluster center

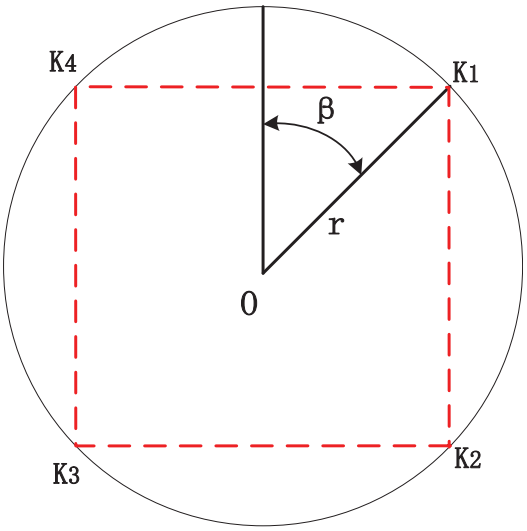

FIGURE 3. The initial cluster center distribution of $K = 4$.

selection method is presented as in formula (4).

$$\begin{cases} C_x^k = \frac{r}{2} + \frac{r}{2} \cdot \sin[(k-1) \cdot \frac{2\pi}{K} + \beta] \\ C_y^k = \frac{r}{2} + \frac{r}{2} \cdot \cos[(k-1) \cdot \frac{2\pi}{K} + \beta] \end{cases} \tag{4}$$

where C_x^k, C_y^k represent the coordinates of the kth initial clustering center K_k, $r = \min(X_{max}, Y_{max})$ and X_{max}, Y_{max} represent the range of map, K is the number of clusters, $\beta = \frac{\pi}{3}$.

As shown in Fig.3, with the center of the map as the center of the circle, the initial cluster centers are evenly distributed around the circle [27].

To address the K-means problem, the simplest approach named Lioyd's algorithm [26] is presented. Once cluster centers are initialized, each point is alternatively assigned to its closest center, and then cluster centers are updated to alternatively minimize the variables in formula (5) until convergence.

$$minE = \sum_{k=1}^{K} \sum_{d \in C_k} ||d - \mu_k||_2^2 \tag{5}$$

where $D = \{d_1, d_2, \cdots d_{N_a}\}$ is sample set of UAV coordinates, $C = \{C_1, C_2, \cdots C_K\}$ is the cluster grouping of UAVs, E is square error of a cluster, $\mu_k = \frac{1}{|C_k|} \sum_{d \in C_k} d$ is the mean vector of C_k.

B. SELECTION OF VITAL COMMUNICATION NODES

The communication topology in a distributed system is usually represented by a graph $G_n = (V, E)$, $V = \{v_1, v_2, \cdots v_n\}$ represents the set of nodes in G_n, $E = \{(v_i, v_j)|v_i, v_j \in V\}$ represents the set of edges in G_n, and $|V| = n = N_a$, $|E| = m$. A is the adjacency matrix of G_n.

$$A_{ij} = \begin{cases} 1 & (v_i, v_j) \in E \\ 0 & \text{otherwise} \end{cases} \tag{6}$$

where $A_{ij} = 1$ represents that there is an edge connection between UAV i and UAV j. In other words, the communication distance between UAV i and UAV j is 1-hop. Otherwise, $A_{ij} = 0$.

Recognition of vital nodes in complex networks retains great importance in the improvement of network's robustness and vulnerability [28]. The prevalently used centrality measures are degree centrality (DC) [29], betweenness centrality (BNC) [30], closeness centrality(CNC) [31] and eigenvector centrality (EVC) [32]. To reduce communication loads, vital communication nodes should cover as many communication nodes as possible within 1-hop communication distance. Based on the indicators mentioned above, a calculation model of UAV vital communication nodes is proposed.

$$\begin{cases} BNC(v_i) = \sum\limits_{s \neq t \neq v_i \in V} \frac{\sigma_{st}(v_i)}{\sigma_{st}} \\ CNC(v_i) = \frac{n-1}{\sum\limits_{j \neq i} d_{ij}} \\ DC(v_i) = \sum\limits_{j=1}^{n} A_{ij} \\ EVC(v_i) = \frac{\sum\limits_{j=1}^{n} A_{ij} c_e(v_j)}{\lambda} \end{cases} \tag{7}$$

where $BNC(v_i)$ is betweenness centrality of UAV i, σ_{st} denotes the number of shortest paths from $s \in V$ to $t \in V$. $\sigma_{st}(v_i)$ denotes the number of shortest paths from s to t that v_i lies on. $CNC(v_i)$ is closeness centrality of UAV i, d_{ij} denotes the distance between v_i and v_j. $DC(v_i)$ is the degree centrality of UAV i, $EVC(v_i)$ is the eigenvector centrality of UAV i, $c_e(v_j)$ is the principal eigenvector and λ is the main eigenvalue.

In the DCCBBA, the importance of communication nodes can be expressed as the normalized mean of the above indicators.

$$Y(v_i) = \frac{BNC(v_i)}{\sqrt{\sum\limits_{i=1}^{n} BNC(v_i)}} + \frac{CNC(v_i)}{\sqrt{\sum\limits_{i=1}^{n} CNC(v_i)}} + \frac{DC(v_i)}{\sqrt{\sum\limits_{i=1}^{n} DC(v_i)}} + \frac{ENC(v_i)}{\sqrt{\sum\limits_{i=1}^{n} ENC(v_i)}} \tag{8}$$

where $Y(v_i)$ is the importance value of node v_i. The UAV with the highest importance value is selected as the vital communication node in a cluster. Besides, if the importance values of two UAVs are the same, the UAV with a smaller label is selected as the vital communication node.

In this paper, the exchange of information between different UAVs through the shortest path is recorded as effective communication. Take Fig.4 as an example, the number of communication events from UAV 1 to UAV 6 is 3, and the number of communication events from UAV 1 to UAV 2 is 1. Therefore, the communication scale is defined

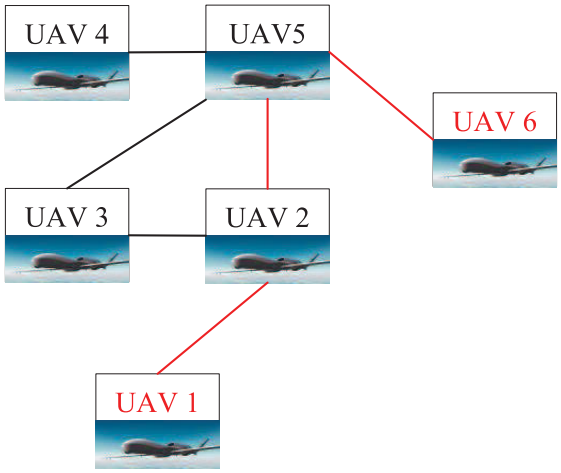

FIGURE 4. An example of calculating the number of communication events.

as the total communication events required for the collective to reach a viable solution, which is an important indicator for measuring the occupation of communication resources in the battlefield [33].

C. BUNDLE CONSTRUCTION PHASE

The proposed DCCBBA is revised based on the baseline CBBA to solve the decentralized task allocation problem with duo cooperation and heterogeneous UAVs. SGA that sequentially finds a sequence of UAV-task pairs that render the largest score values given prior selections has been analyzed in [7]. In the bundle construction phase of DCCBBA, SGA is applied to add tasks to b_i and p_i. In addition, Z_i and Y_i are carried to find a conflict-free assignment with complex constraints, which can be expressed as follows.

(1) Z_i represents the winning UAV matrix, which is a $N_a \times N_T$ matrix. The element $z_{kj}^i = 1$ in Z_i denotes that UAV i consider UAV k the winner for bidding task j. Otherwise, $z_{kj}^i = 0$. Furthermore, $\sum_{k=1}^{N_a} z_{kj}^i$ is the total number of UAVs considered as winners for bidding task j by UAV i.

(2) Y_i represents the winner bid value matrix, which stores the bidding values from the perspective of UAV i. Each element in Y_i corresponds to Z_i one by one. The element $y_{kj}^i = 1$ in Y_i denotes that the bid value of UAV k for task j considered by UAV i.

In the bundle construction phase of DCCBBA, tasks are added to UAV i's bundle until UAV i is incapable of adding any other task. If $num_j = 1$, the task j can be accomplished by a single UAV and assignment of additional UAV is unacceptable. Otherwise, the task j must be accomplished by cooperation of multiple UAVs. When the number of UAVs bidding for task j has met the requirement, that is, $\sum_{k=1}^{N_a} z_{kj}^i = num_j$, the UAV i compares c_{ij} with the minimum winning bid value $\min(y_{kj}^i)$ for task j. If $c_{ij} > \min(y_{kj}^i)$, $\forall k \in N_a$, UAV i can bid for task j, otherwise UAV i abandons task j. The procedure of UAV i's bundle construction of DCCBBA is presented in Algorithm 2.

Algorithm 2 Bundle Construction Phase of DCCBBA for UAV i at Iteration t

Input : $b_i(t-1), y_i(t-1), p_i(t-1), z_i(t-1)$
Out : $b_i(t), y_i(t), p_i(t), z_i(t)$
1 : $b_i(t) = b_i(t-1), y_i(t) = y_i(t-1), p_i(t) = p_i(t-1), z_i(t) = z_i(t-1)$
2 : for $j = 1 : N_T$
3 : if $j \in b_i$
4 : $c_{ij} = 0$
5 : $x_{ij} = 0$
6 : else
7 : $c_{ij} = \max_{n \le |p_i|} S_i^{p_i \oplus_n \{j\}} - S_i^{p_i} \quad \forall j \notin b_i$
8 : if $num_j > \sum_{k=1}^{N_a} z_{kj}^i$
9 : $x_{ij} = 1$
10 : else
11 : if $c_{ij} > \min(y_{kj}^i)$
12 : $x_{ij} = 1$
13 : else
14 : $x_{ij} = 0$
15 : end if
16 : end if
17 : end if
18 : if constraints in eqs. (2) are satisfied
19 : while $|b_i(t-1)| < L^i$
20 : $C_j = \arg\max_j (c_{ij} \cdot x_{ij})$
21 : $n_{ij} = \arg\max_n S_i^{p_i \oplus_n \{C_j\}}$
22 : $b_i = b_i \oplus_{end} \{C_j\}, p_i = p_i \oplus_{n_{ij}} \{C_j\}$
23 : $y_{iC_j} = c_{iC_j}, z_{iC_j} = 1$
24 : end while
25 : end if
26 : end for

In lines 4-5 of algorithm 2, if the task j is already included in b_i, it provides no additional improvement in the reward. In lines 8-16, whether UAV i can participate in the bidding for task j is considered. In line 18, only UAVs that are capable of performing and simultaneously satisfying the task precedence constraint in eqs.(2) can bid for task j.

D. INNER CONFLICT RESOLUTION PHASE

In the inner conflict resolution phase, the consensus strategy is improved to handle the violated task assignment between UAVs that belongs to the same cluster. The UAVs in a cluster only need to communicate with the corresponding vital communication node through the shortest path, thus total communication can be reduced compared with the baseline CBBA. As shown in Fig.5, UAV 1 is selected as the vital communication node in a cluster, UAV 2, UAV 5 and UAV 6 can communicate directly with UAV 1, while UAV 3 and UAV 4 can communicate with UAV 1 through UAV 2.

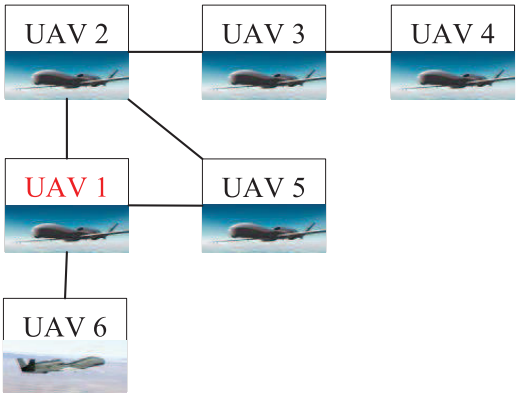

FIGURE 5. Internal communication diagram in a cluster.

To further ease the communication traffic in the inner conflict resolution phase, communication with all adjacent UAVs is not necessary. For example, the communication between UAV 2 and UAV 5 will not produce any useful information, but also cause a certain degree of communication redundancy in Fig.5. Besides, multiple UAVs, which are not in conflict with other UAVs participating in the communication may increase network load. For instance, the baseline CBBA requires UAV 1 and UAV 6 to conduct two-way communication on each task, including the task information that UAV 1 does not need. In the DCCBBA, UAV 1 serves as the receiver to save the information of UAV 6 if UAV 1 is not in conflict with UAV 6 for a task.

The phase of inner conflict resolution is summarized and detailed in Algorithm 3.

In algorithm 3, T_i is a collection of UAVs. First, UAV i compares the winning bid information for task j with UAV k to make sure its information is up to date (lines 2-5). $s_{km} > s_{im}$ indicates that the information of UAV k is latest (line 4). UAV i updates z^i_{kj} and y^i_{kj} based on the comparison results (line 5). Second, if the number of UAVs bidding for tasks j considered by UAV i has not met the requirement, z^i_{kj} and y^i_{kj} are updated in lines 7-9. Otherwise, UAV i compares $\min(y^i_{nj} \forall n \in T_i)$ with y^k_{mj} to update the information of UAV n and UAV i in lines 9-15. Finally, UAV i serves as the receiver to save the information of UAV k if UAV i is not in conflict with UAV k for tasks j in lines 18-22.

E. OUTER CONFLICT RESOLUTION PHASE

Conflicts in a cluster can be reduced in the inner conflict resolution phase, but it does not guarantee conflict-free assignments in the overall UAVs. Each vital communication node in a cluster exchanges messages with vital a communication node which belongs to another cluster and is connected. The external communication diagram between clusters is shown in Fig.6.

In this process, consensus for the entire UAVs can be achieved by exchanging messages between vital communication nodes. After the outer conflict resolution phase,

Algorithm 3 Inner Conflict Resolution Phase of DCCBBA at Iteration t

UAV k sends $y_k(t-1), z_k(t-1), s_k(t-1)$ to UAV i while UAV i
is the vital communication node in the cluster C_i,
$T_i = T_i \cup \{k\} \quad T_i \subset C_i$
Input : $y_k(t-1), z_k(t-1), s_k(t-1)$
Out : $y_i(t), z_i(t), s_i(t)$
1 : *for* $\forall j \in N_T$
2 : if $z^i_{mj} = 1 \quad \forall m \in C_i$
3 : if $z^k_{mj} = 1$
4 : if $m = k \quad \& \quad s_{km} > s_{im}$
5 : $z^i_{kj} = 1, y^i_{kj} = y^k_{mj}$
6 : else
7 : if $\sum_{m=1}^{T_i} z^i_{mj} < num_j$
8 : $z^i_{kj} = 1, y^i_{kj} = y^k_{mj}$
9 : else
10 : if $\min(y^i_{nj} \forall n \in T_i) < y^k_{mj}$
11 : $z^i_{nj} = 0, y^i_{nj} = 0$
12 : *release task n and tasks added after it*
13 : $z^i_{kj} = 1, y^i_{kj} = y^k_{mj}$
14 : end if
15 : end if
16 : end if
17 : end if
18 : else
19 : if $z^k_{mj} = 1$
20 : $z^i_{kj} = 1, y^i_{kj} = y^k_{mj}$
21 : end if
22 : end if
23 : end for

each key communication node broadcasts task assignments to other UAVs in the same cluster. Therefore, each UAV shares the same situation awareness and conflict-free assignments can be guaranteed. The phase of outer conflict resolution is described in Algorithm 4.

In lines 2-6 of algorithm 4, UAV i compares the winning bid information for task j with UAV k to make sure its information is up to date. In lines 8-11, if the number of UAVs bidding for tasks j considered by UAV i has not met the requirement, z^i_{mj} and y^i_{mj} are updated when UAV k consider UAV $m (m \neq i)$ perform task j while UAV i believes UAV m does not execute task j. Otherwise, UAV i compares $\min(y^i_{nj} \forall n \in C_i \cup C_k)$ with y^k_{mj} to update the information of UAV n and UAV i in lines 12-16.

F. PATH PLANNING BASED ON PH CURVES

Pythagorean hodograph curves (PH curves) have a number of advantages over other splines commonly used in planar robot path planning [34], [35], [36]. A brief introduction of the PH path is given in the section, the detailed one can be found in [34]. In this paper, a fifth order PH curve is used

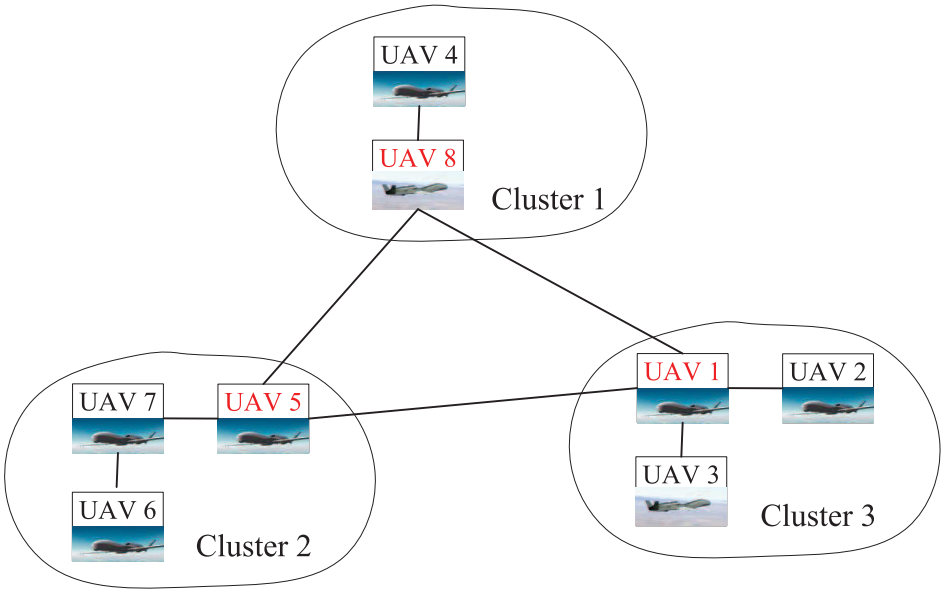

FIGURE 6. External communication diagram between clusters.

Algorithm 4 Outer Conflict Resolution Phase of DCCBBA for UAV i at Iteration t

UAV k sends $y_k(t-1), z_k(t-1), s_k(t-1)$ to UAV i while UAV i
and UAV k are the vital communication nodes in cluster C_i and cluster C_k
Input : $y_k(t-1), z_k(t-1), s_k(t-1)$
Out : $y_i(t), z_i(t), s_i(t)$

```
for ∀j ∈ N_T
    for ∀m ∈ C_i ∪ C_k & z^i_mj = 1
        if k = m & s_km > s_im
            z^i_mj = z^k_mj, y^i_mj = y^k_mj
        end if
    end for
    for ∀m ∈ C_i ∪ C_k & z^k_mj = 1
        if m ≠ i & z^i_mj = 0 & s_km > s_im
            if Σ_{m=1}^{C_i∪C_k} z^i_mj < num_j
                z^i_mj = z^k_mj, y^i_mj = y^k_mj
            else
                if z^k_j ≠ 0 & y^k_j ≠ 0
                    if min(y^i_nj ∀n ∈ C_i ∪ C_k) < y^k_mj
                        z^i_nj = 0, y^i_nj = 0
                        release task n and tasks added after it
                        z^i_mj = z^k_mj, y^i_mj = y^k_mj
                    end if
                end if
            end if
        end if
    end for
end for
```

as it has inflection points that provide sufficient flexibility. A fifth order Bernstein-Bęzier polynomial can be expressed as formula (9)-(11).

$$r(q) = \sum_{k=0}^{5} b_k \binom{5}{k} (1-q)^{(5-k)} q^k \tag{9}$$

$$\binom{5}{k} = \frac{5!}{5!(5-k)!} \tag{10}$$

$$s(q) = \int_{q_1}^{q_2} r(q)dq \quad q_1, q_2 \in [0,1] \tag{11}$$

where b_k is the kth control point $k \in [1,2,3,4,5]$, whose vertices define the control polygon or Bęzier polygon. $r(q)$ is the path point, $q \in [0,1]$ is the normalized path parameter, $s(q)$ is the length of the carve.

The four control points of the Bęzier polygon can be calculated by the first order Hermite interpolation while the initial and final positions and directions are considered [37].

$$\begin{aligned} b_0 &= (x_s, y_s) \\ b_5 &= (x_f, y_f) \\ d_0 &= M(cos\phi_s, sin\phi_s) \\ d_5 &= N(cos\phi_f, sin\phi_f) \\ b_1 &= b_0 + \frac{1}{5}d_0 \\ b_4 &= b_5 - \frac{1}{5}d_5 \end{aligned} \tag{12}$$

where (x_s, y_s) is initial position, (ϕ_s, β_s) is the initial orientation, (x_f, y_f) is final position, (ϕ_f, β_f) is the final orientation, d_0 and d_5 are initial and final direction, M and N are positive constants.

It is assumed that UAVs fly at a fixed altitude, the kinematic model of the UAV can be expressed as formula (13)

$$\begin{bmatrix} \dot{x} \\ \dot{y} \\ \dot{\chi} \end{bmatrix} = \begin{bmatrix} \cos\chi & 0 \\ \sin\chi & 0 \\ 0 & 1 \end{bmatrix} \begin{bmatrix} v \\ \omega_\chi \end{bmatrix} \tag{13}$$

where $\dot{x}, \dot{y}$ represent the velocity in the x and y directions respectively, v is the flight speed, χ is the heading angle, $\dot{\chi}$ is the angular velocity of heading angle.

V. PERFORMANCE ANALYSIS OF DCCBBA

A. COMMUNICATION LOAD ANALYSIS

To keep the collective up to date, an increase in the number of participating UAVs or tasks leads to an exponential communication events in baseline CBBA [7]. Moreover, each UAV sends local assignment information to other UAVs while receiving information from them. If the network between UAVs is fully connected, the number of communication events in baseline CBBA can be expressed as follows [16].

$$T_b = C_b \cdot N_a \cdot (N_a - 1) \tag{14}$$

where T_b is the total communication events in CBBA, C_b is the number of baseline CBBA rounds required for UAVs to reach a viable solution.

Compared with the baseline CBBA, the proposed DCBBA can significantly reduce the number of communication events required to achieve consensus with fully connected. The number of communication events in DCCBBA can be expressed as formula (15).

$$T_d = C_d \cdot (2(N_a - K) + K \cdot (K - 1)/2) \tag{15}$$

where T_d is the total communication events in DCCBBA, C_d is the number of DCCBBA rounds, $N_a - K$ represents the communication events between UAVs and vital communication nodes in inner conflict resolution phase, $K(K-1)/2$ represents the communication events between vital communication nodes in outer conflict resolution phase. To share the same situation awareness between UAVs, $N_a - K$ communication events are needed after the outer conflict resolution phase in a round.

B. CONVERGENCE ANALYSIS

In this section, the convergence of DCCBBA is presented, where convergence means producing an assignment in finite time with all constraints in eqs.(2) being satisfied. As point out in [7], CBBA converges to a conflict-free assignment scoring scheme satisfied the diminishing marginal gain(DMG) property.

Consider the DCCBBA process with synchronous conflict resoluction over a static network with diameter D for the case that every UAV's scoring scheme is DMG. The following holds.

(1)The time required for inner conflict resolution for cluster $C_i, \forall i \in K$ is bound by D_{C_i}, D_{C_i} is the network diameter of C_i.

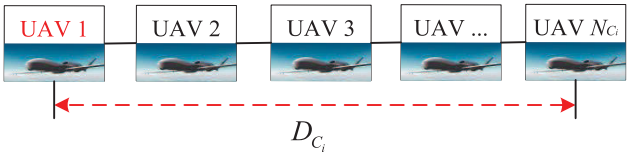

FIGURE 7. An example to illustrate the worst-case performance in inner conflict resolution.

(2)The convergence time of outer conflict resolution is bound by $K \cdot D$.

Proof for (1)

If the inner conflict resolution is assumed to be synchronized, i.e, each UAV in a cluster exchanges messages with the vital communication node through the shortest path in the tth iteration simultaneously. In this case, the time can be defined as the shortest time where all UAVs in a cluster exchange information with vital communication node. The maximum communication time required for the baseline CBBA is $N_{min} \cdot D, N_{min} = min(N_a L_i, N_T), i \in [1, N_a]$. Applying this result to the inner conflict resolution of DCCBBA, the convergence time of the inner resolution is D_{C_i}. The worst-case performance in inner conflict resolution can be shown in Fig. 7.

In Fig.7, take chain communication network as an example, UAV 1 is vital communication node in a cluster, the network diameter D_{C_i} is defined as the longest of all the shortest path lengths from UAV_{N_c} to UAV 1.

Proof for (2)

Outer conflict resolution phase can guarantee conflict-free assignments in the overall UAVs. The time for the outer conflict resolution phase in a round is bounded by the diameter D. To find conflict-free assignments, the outer conflict resolution phase should be repeatedly performed between vital communication nodes. The worst-case performance is that all vital communication nodes bid on the same tasks in every round. All vital communication nodes except one vital communication node will release those tasks in a round. A maximum of K times is required to perform the outer conflict resolution repeatedly to eliminate conflicts between vital communication nodes. Therefore, the convergence time of outer conflict resolution is bound by $K \cdot D$.

C. COMPLEXITY ANALYSIS

In this section, the computational complexities of different algorithms generated by the DCCBBA are analyzed, demonstrating its performance from the theoretical perspective. Simple instructions in each algorithm are omitted, which do not really affect the computational complexity of the algorithm [10]. For clarity, each algorithm is elaborated separately.

1) GENERATION OF CLUSTERS

Predetermined clustering clusters of K-means algorithm are produced using equation (4) in section IV-A. The standard K-means algorithm has a computational complexity

of $O(n \cdot k \cdot l)$ [38] because of the iterative nature, where l is the number of iterations, k is the number of clusters and n is the number of data-points. Therefore, the computational complexity of this algorithm is $O(N_a \cdot K \cdot C_d)$.

2) SELECTION OF VITAL COMMUNICATION NODES

This algorithm contains one elementary instruction. The UAV with the highest importance value is selected using equation (8) as the vital communication node in a cluster. Therefore, the computational complexity of this algorithm is $O(1)$.

3) BUNDLE CONSTRUCTION PHASE

As shown in Algorithm 2, bundle construction phase contains two blocs of nested loops and several elementary instructions. It starts at line 2 and ends at line 26. The worst-case computational complexity is $O(N_T \cdot L^i)$.

4) INNER CONFLICT RESOLUTION PHASE

As shown in Algorithm 3, inner conflict resolution phase contains two blocs of nested loops and several elementary instructions. The bloc starts at line 1 and ends at line 23. Its computational complexity is $O(N_T)$.

5) OUTER CONFLICT RESOLUTION PHASE

As shown in Algorithm 4, outer conflict resolution contains one bloc of nested loops. The bloc is presented in lines 1-22. It contains two blocs of nested loops and several elementary instructions. The worst computational complexity of the first bloc is $O(N_T)$, which starts at line 2 and ends at line 6. Similarly, the worst computational complexity of other block shown in lines 7-21 is $O(N_T)$. Therefore, the worst computational complexity of outer conflict resolution is $O(N_T \cdot (N_T + N_T))$.

In conclusion, the worst computational complexity of DCCBBA is $O(N_a \cdot {N_T}^3)$. According to [10], it is worth pointing out that approximately one second is taken to perform $f(1000)$ operations by a CPU, which can execute one billion of operations per second.(f is a given algorithm).

VI. SIMULATIONS

The simulation results for DCCBBA are presented in this section to illustrate its effective and outstanding performance. To describe the performance of the proposed DCCBBA, the baseline CBBA [7], CF-CBBA [16], G-CBBA [20] and Two-layer CBBA [18] are introduced as the compared methods. Numerical simulations are conducted comparing with the existing methods. In this paper, the locations of the tasks and UAVs are given at the beginning and no dynamic changes during the whole process. Monte-Carlo simulations are run for six different scenarios.

All the simulations are adopted in Matlab environment on a PC equipped with Intel (R) Core (TM) i7-8700 CPU@3.20GHZ, the memory is 16.0 GB, and the system is Windows 11 Professional system.

TABLE 2. Parameters of heterogeneous UAVs.

UAV ID	Type	L_t	Velocity(m/s)	Initial position(m)	D_t^{limit} (km)
U_1	reconnaissance	5	80-200	(2000,0)	30
U_2	reconnaissance	5	80-200	(4000,0)	30
U_3	strike	5	100-200	(6000,0)	30
U_4	strike	5	100-200	(8000,0)	30

TABLE 3. Parameters of tasks.

Task ID	Type	Time window(s)	Task duration(s)
$T_1 - T_2$	reconnaissance	[0,300]	5
$T_3 - T_5$	strike	[0,300]	5
$T_6 - T_8$	*R&S*	[0,300]	5+5

A. FEASIBILITY OF DCCBBA

In the scenario, there are $N_a = 10$ tasks marked $T_1 - T_{10}$ and $N_T = 4$ heterogeneous UAVs marked $U_1 - U_4$ within a 10 kmx10 km rectangular area. The three task types are reconnaissance, strike, integrated reconnaissance and strike task (*R&S*). $T_1 - T_2$ are reconnaissance tasks, one UAV with reconnaissance capability is required to accomplish a reconnaissance task. $T_3 - T_5$ are strike tasks, two UAVs with strike capability are needed to accomplish a strike task simultaneously. $T_6 - T_8$ are *R&S* tasks, which require one UAV with reconnaissance capability first and one UAV with strike capability when the reconnaissance subtask j is finished. Besides, tasks are set with a time-discounted score in the form of $c = 1000 \cdot \exp(-0.01 \cdot t)$. The initial positions of all tasks are generated in a random manner and all tasks have a time window [0,300] s.

Moreover, it is assumed that the collective network is fully connected mesh. Parameters of heterogeneous UAVs and tasks are exhibited in TABLE 2 and TABLE 3.

The task schedules of UAVs are shown in Fig. 8

As shown in Fig. 8, the red line, green line, blue line and black line represent the performing sequence of $U_1 - U_4$ respectively, while the square and circle marks separately represent tasks and UAVs. The performance of DCCBBA presented in Fig. 8(a) meets task allocation requirements and the paths are closer to flyable paths due to PH curves. In contrast, regarding the task assignment solution without considering path planning in Fig. 8(b) satisfies the constraints, the paths are not smooth at all, which will lead to the inconsistency between the route cost obtained from the task allocation and the actual route cost. The difference of total path length between Fig. 8(a) and Fig. 8(b) in the scenario is 9.03%.

The time schedules of UAVs are shown in Fig. 9.

In Fig. 9, task allocation results meet time window constraints. Besides, UAVs can arrive simultaneously for $T_3 - T_5$ by changing the velocity. According to Fig.8 and Fig.9, the task assignments for UAVs are exhibited in TABLE 3.

As shown in TABLE 4, the task assignments are conflict-free, which meet the constraints of the time window and UAVs capabilities. The change of UAV clustering number is

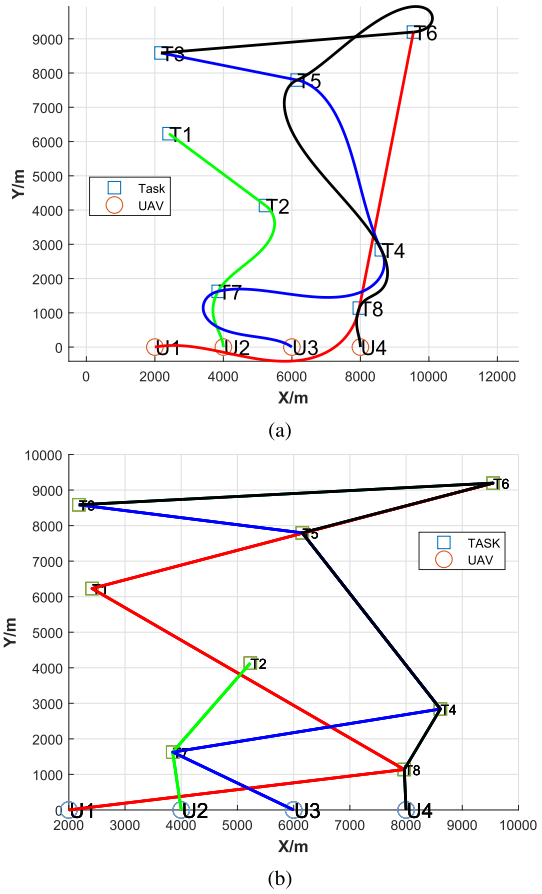

FIGURE 8. The task schedules of UAVs. (a) task assignments using DCCBBA, (b)task assignments without considering path planning.

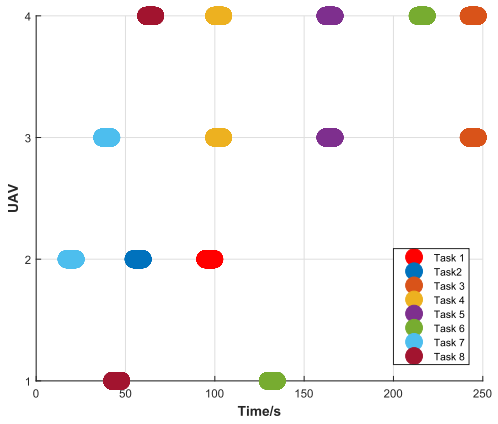

FIGURE 9. The task schedules and time schedules of UAVs using DCCBBA.

shown in Fig. 10 and communication events in each iteration are exhibited in Fig. 11.

As shown in Fig.10 and Fig.11, the DCCBBA converges after five iterations, the total number of communication events in inner conflict resolution phase is 6 while the number of communication events in outer conflict resolution phase is 15. The number of communication events is consistent with the analysis in section V. Generally speaking, conflict-free

TABLE 4. Task assignments for heterogeneous UAVs.

UAV ID	Tasks schedules	Performing time of task(s)	Voyage (km)	Total reward
U_1	T_8, T_6	42.54, 129.66	14.97	926.95
U_2	T_7, T_2, T_1	17.04, 54.57, 94.68	8.47	1810.74
U_3	T_7, T_4, T_5, T_3	37.02, 99.64, 161.98, 242.15	19.25	1346.49
U_4	T_8, T_4, T_5, T_6, T_3	61.58, 99.64, 161.98, 213.58, 242.15	22.22	1314.28

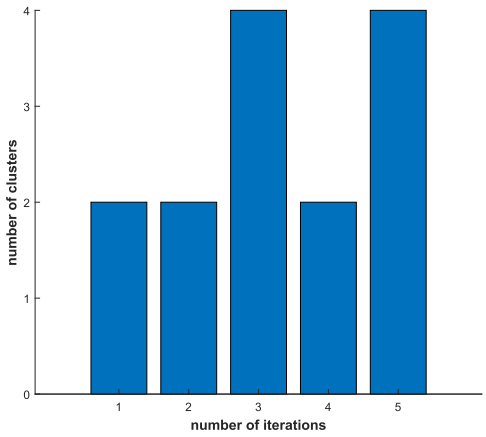

FIGURE 10. The change of UAV clustering number.

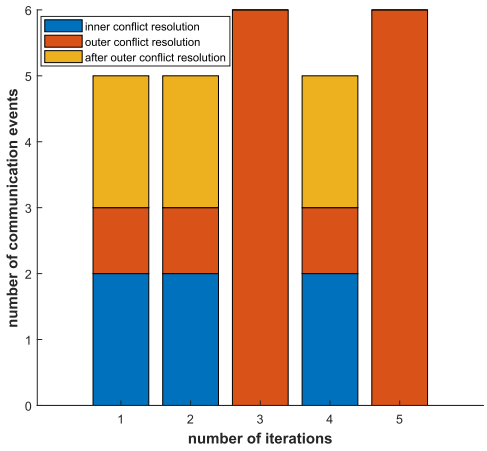

FIGURE 11. Communication events in each iteration.

assignments can be obtained with all constraints in eqs.(2) being satisfied, indicating that the DCCBBA can solve the UAV task allocation problem with complex constraints.

B. ALGORITHM VALIDATION

To illustrate the superiority of the proposed DCCBBA, the baseline CBBA, CF-CBBA, GCBBA are introduced as the compared methods in this section. Scenario of increasing number of tasks using eight homogeneous UAVs with fully connected network is presented. The $N_T = 8$ heterogeneous UAVs and tasks are randomly generated in the designed

area, the maximum number of tasks each UAV can perform $L_t = 10$. What is more, the performances of algorithms are analyzed by running one hundred Monte-Carlo simulations for each scenario. The results of the comparisons between DCCBBA and baseline CBBA, CFCBBA, GCBBA are shown in Fig.12.

Fig.12(a) shows the communication events of the four methods. As the number of tasks increases, the total communication events required to drive task allocation to convergence increases slightly. The CF-CBBA requires the least number of communication events due to the simple algorithm structure. However, the CF-CBBA gives the lowest performance in total reward presented in Fig.12(b) and the highest allocation failures presented in Fig.12(c). Conversely, DCCBBA shows benefit for allocation failures and little difference in total reward with baseline CBBA and GCBBA. The reason is that the number of clusters is randomly generated between 1 and N_a, and the dynamic clustering method is adopted in DCCBBA, which enables sufficient consistency processing between UAVs. Therefore, the number of DCCBBA failures is significantly lower in Fig.12(c). What's more, compared with baseline CBBA and GCBBA, the number of communication events of DCCBBA is significantly lower due to the fact that each UAV only need to communicate with the vital communication node in the same cluster. Apart from that, communication events between vital communication nodes are needed while each UAV needs communicate with all the UAVs theoretically in the baseline CBBA.

The number of communication events in DCCBBA is shown in Fig.13.

As the number of tasks increases, the communication events in inner conflict resolution and outer conflict resolution have an increasing tendency for agreement between UAVs. The reason is that more communication hops are required to obtain conflict-free assignments between UAVs, which is consistent with the analysis in section V.

C. DIFFERENT COMMUNICATION TOPOLOGIES

The section presents the simulation results of the DCCBBA to illustrate that the proposed method is applicable to different communication networks. Given the nature of the distributed task allocation, six basic communication topologies [24], [39] with ten heterogeneous UAVs varying a number of *R&S* tasks between 5 to 30 are tested for the proposed DCCBBA. The shape of communication networks are shown in Fig.14. Besides, the maximum number of tasks each UAV can perform $L_t = 10$, UAVs and tasks locations are randomly generated in the design area. The performance of algorithms are analyzed by running one hundred Monte-Carlo simulations for each scenario. For each set of examples, the communication events and number of clusters are compared and analyzed. Other parameters of heterogeneous UAVs and tasks are the same as those in section VI-A.

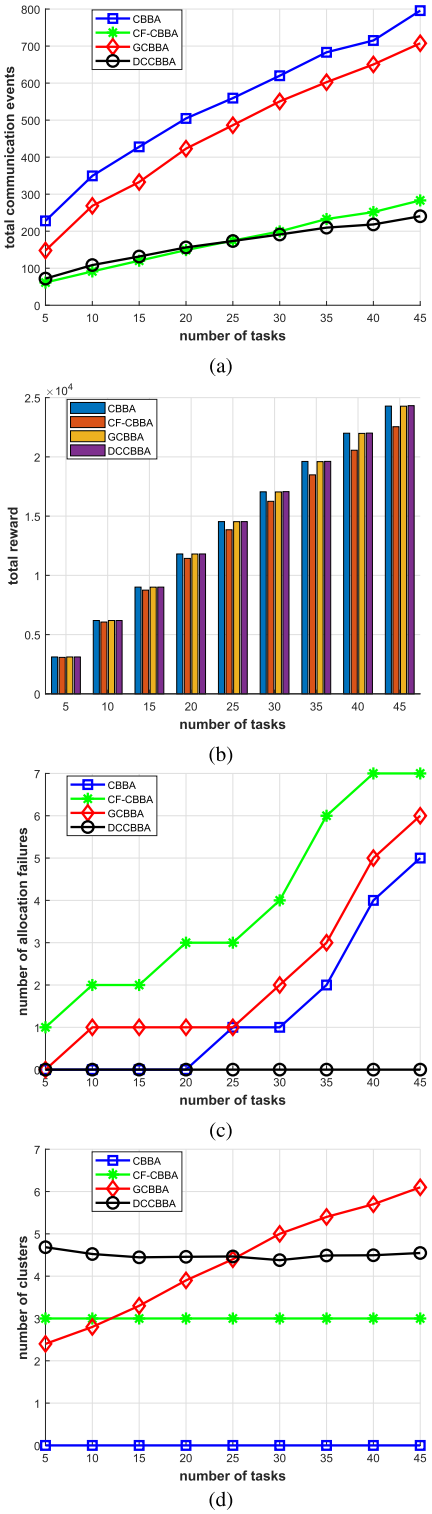

FIGURE 12. Results of the comparisons between DCCBBA and compared methods. (a) total communication events, (b) total reward, (c) number of allocation failures, (d) number of clusters.

For every case when N_T remains unchanged, it should be noted that the task assignment result is the same. Task assignment result in $N_a = 10$, $N_T = 15$ is shown in Fig. 15.

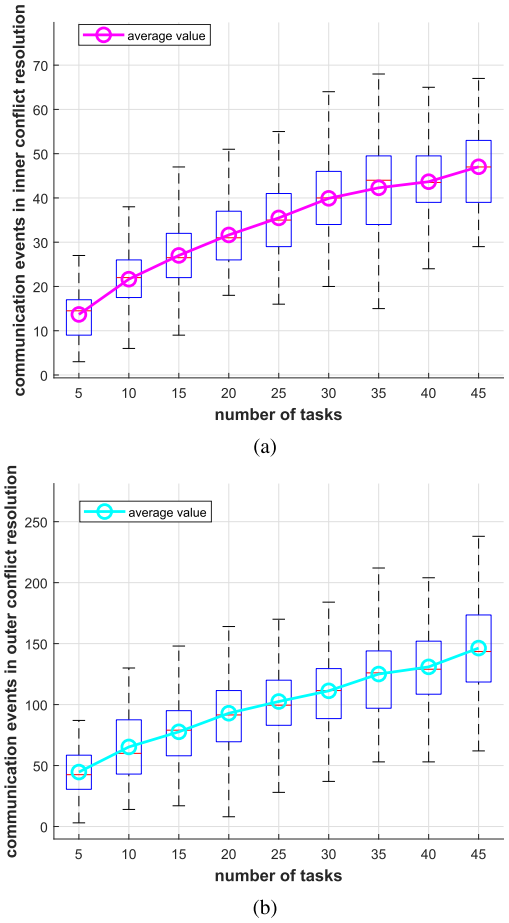

FIGURE 13. The number of communication events in DCCBBA. (a) communication events in inner conflict resolution, (b) communication events in outer conflict resolution.

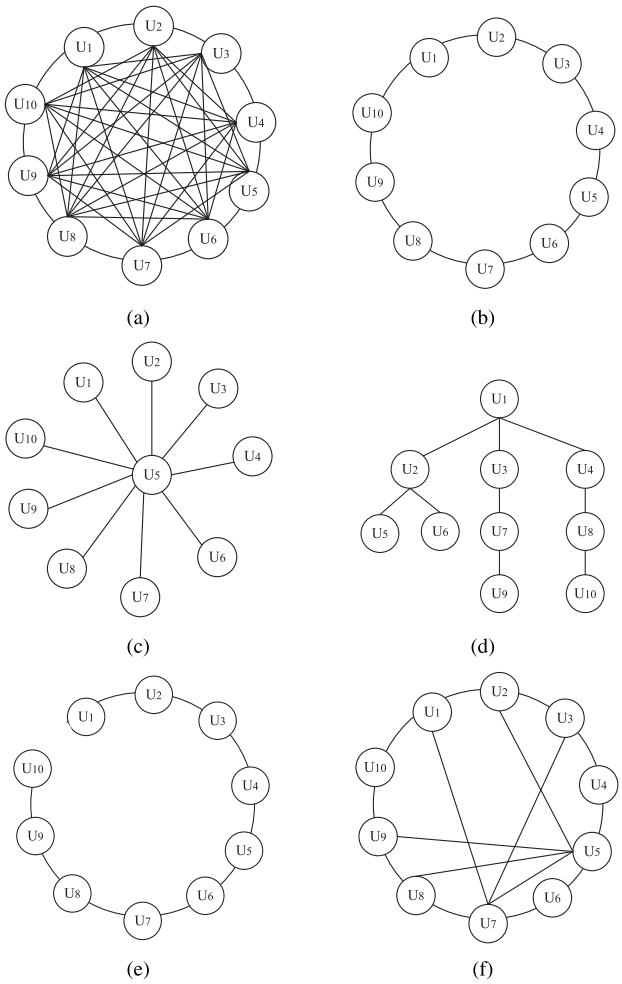

FIGURE 14. Shape of communication networks. (a) Full, (b) Ring, (c) Star, (d) Tree, (e) Chain, (f) Dense.

According to the Fig.15 and Fig.16, the communication events of fully connected network required to find a conflict-free matching of coupling tasks to UAVs are significantly lower while the communication events of chain network is the highest. This is due to the fact that all UAVs can communicate with vital communication nodes within one hop in fully connected network. As the number of tasks increases, the mean communication events in inner and outer conflict resolution increases slightly in Fig.16, because the resolution of conflicts between UAVs increases. The average range number of clusters generated randomly in [1,10] is [5.2,5.8] in the scenario, which satisfies the requirement.

D. DIFFERENT COMMUNICATION DENSE

To further illustrate that DCCBBA can effectively reduce communication events between UAVs in different communication networks, the baseline CBBA,GCBBA, Two-layer CBBA are introduced as compared methods in this section. Supposed that $N_a = 10$ heterogeneous UAVs are assigned to perform $N_T = 20$ *R&S* tasks, Other parameters of heterogeneous UAVs and tasks are the same as those in section VI-C. In this paper, the ratio of non-zero elements in the adjacency matrix A_{ij} to $N_a(N_a - 1)$ is used to judge the density of the communication network [40]

$$\rho = \frac{\sum A_{ij}}{N_a(N_a - 1)} \tag{16}$$

where ρ is the communication network density. In the scenario, five communication network structures with different density are selected in Fig. 17.

Fig. 18 shows the one hundred Monte Carlo results under different network density. This is the case that the network density increases 0.2 to 1.0, and the number of tasks and the number of UAVs are constant. First, with the increase of communication network density, the total communication events are reduced. This result is expected because the fewer communication hops are required to arrive at a solution between UAVs in a communication network with higher density. Second, compared with the baseline CBBA, DCCBBA can effectively reduce communication events by at least 48%, and it could be up to 80%. The benefit tends to be more significant when the network density is higher, which is due to the fact that the UAVs in a cluster only need to communicate with the corresponding vital

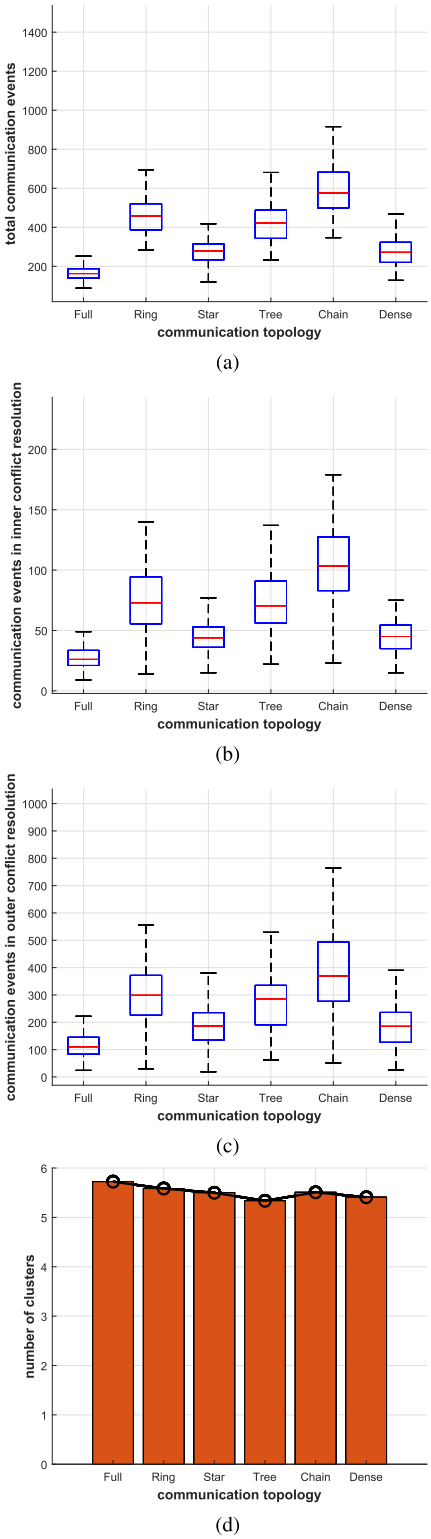

FIGURE 15. $N_a = 10$ heterogeneous UAVs perform $N_T = 15$ *R&S* tasks. (a) total communication events, (b) communication events in inner conflict resolution, (c) communication events in outer conflict resolution, (d) number of clusters.

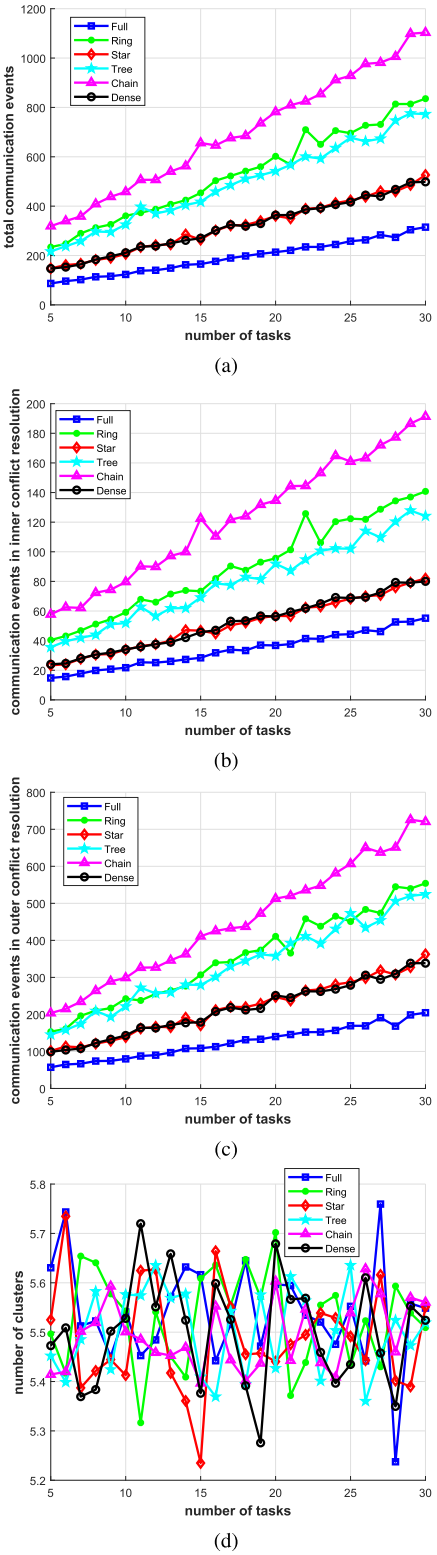

FIGURE 16. $N_a = 10$ heterogeneous UAVs perform $N_T \in [5, 30]$ *R&S* tasks. (a) total communication events, (b) communication events in inner conflict resolution, (c) communication events in outer conflict resolution, (d) number of clusters.

communication node. Apart from that, communication with all adjacent UAVs is not necessary, which can further ease the communication traffic in DCCBBA. Therefore, DCCBBA has better comprehensive performance than baseline CBBA and Two-layer CBBA under this circumstance.

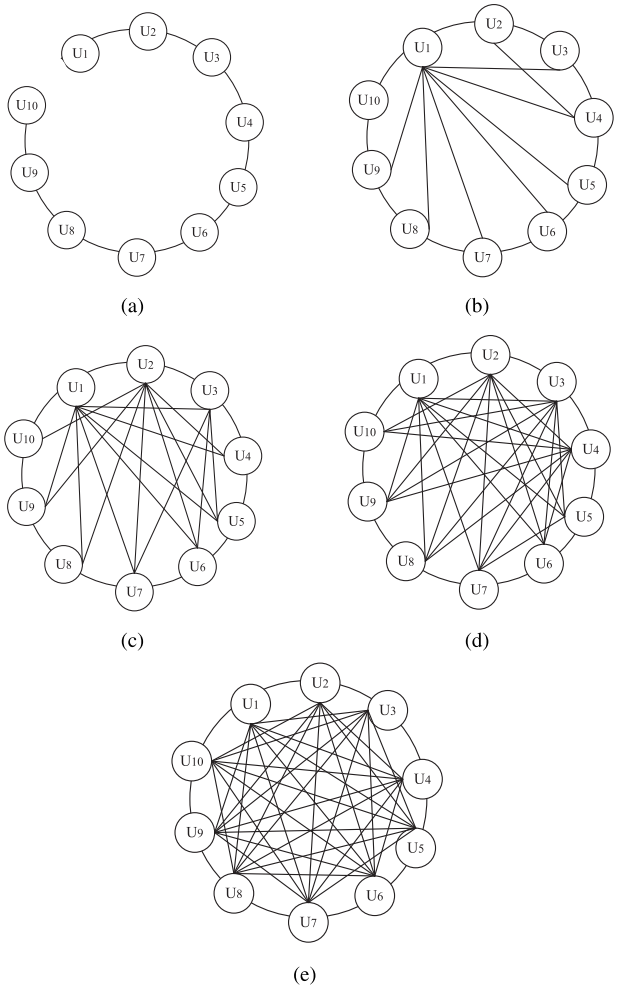

FIGURE 17. Different network density. (a) $\rho = 0.2$, (b) $\rho = 0.4$, (c) $\rho = 0.6$, (d) $\rho = 0.8$, (e)$\rho = 1.0$.

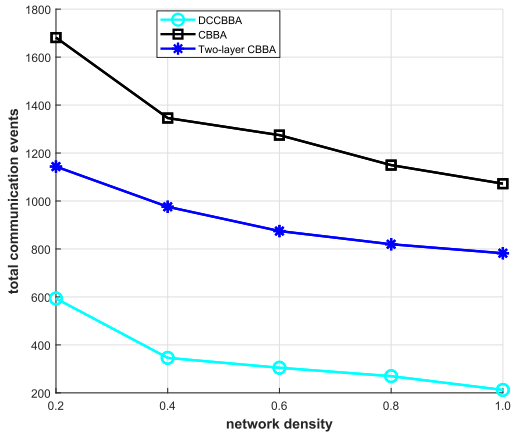

FIGURE 18. Total communication events with different network density.

Fig.19 shows the communication events in inner and outer conflict resolution of DCCBBA for different network density. It can be seen that communication events required to find conflict-free assignments significantly decreases, especially when the network density is lower. The reason for Fig.19 is that more communication hops are required when the network density is lower.

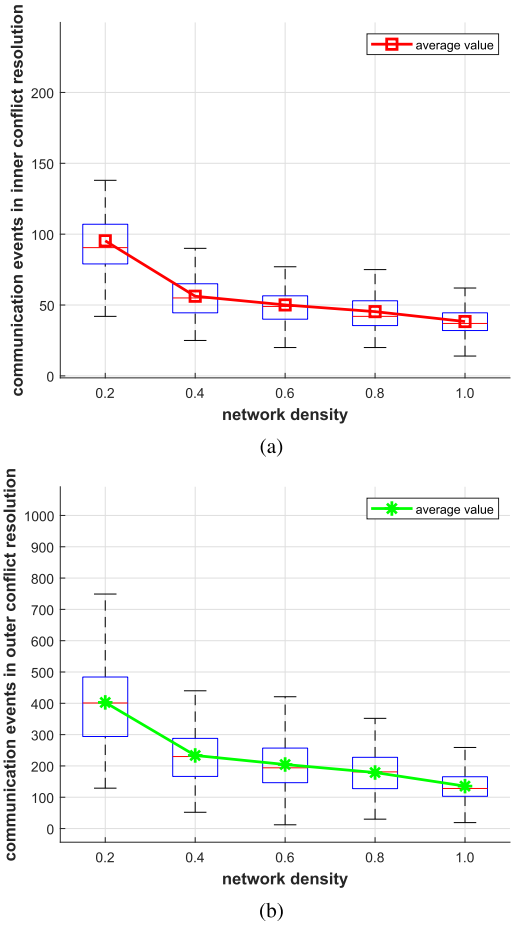

FIGURE 19. Communication events of DCCBBA with different network density. (a) communication events in inner conflict resolution, (b) communication events in outer conflict resolution.

E. DIFFERENT NUMBER OF CLUSTERS

To further analyze the performance of DCCBBA with different number of clusters, one hundred Monte-Carlo simulations are implemented, utilizing the same communication networks described in section VI-C. Scenario of varying a number of clusters between 1 and 10 is presented. Supposed that $N_a = 10$ heterogeneous UAVs are assigned to perform $N_T = 20$ *R&S* tasks. Besides, other parameters of heterogeneous UAVs and tasks are the same as those in section VI-C. The mean performance of DCCBBA under one hundred Monte-Carlo simulations is compared and presented in Fig. 20.

Fig. 20 shows how communication events change as K increases while N_a and N_T stay the same. The results show several interesting things about DCCBBA. First, as seen in Fig. 20(b) and Fig. 20(c), when K varies from 1 to 10, the inner communication events decrease gradually while the outer communication events increase significantly, this is because that outer communication events are exponential with K and inner communication events are linear

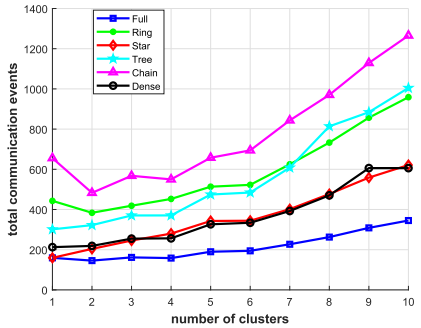

(a)

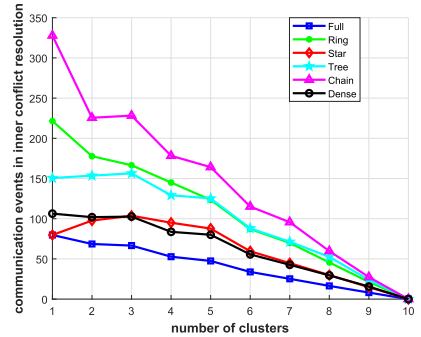

(b)

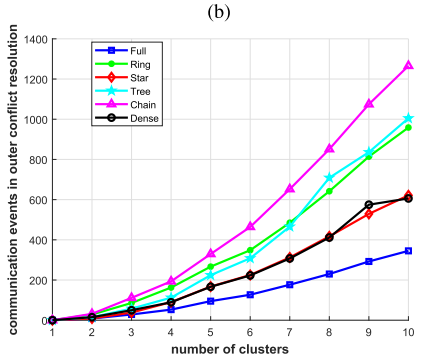

(c)

FIGURE 20. The number of clusters $K \in [1, 10]$ when $N_a = 10$ heterogeneous UAVs perform $N_T = 20$ *R&S* tasks. (a) total communication events, (b) communication events in inner conflict resolution, (c) communication events in outer conflict resolution.

with K in equation (15). Specially, total communication events are equal to inner communication events because communication events only exist within the cluster when $K = 1$ in Fig. 20(c). Similarly, inner communication events are not required when $K = N_a$ in Fig. 20(b). Second, the total communication events required to find conflict-free assignments increase on the whole. It is easy to understand because a high value of K indicates that the outer communication events have a more impact on the total communication events. Furthermore, the communication events of fully connected network are significantly lower than chain networks, which is consistent with the analysis in section VI-C.

F. DIFFERENT NUMBER OF UAVS

To illustrate the impact of increasing number of UAVs, suppose that there are $N_a \in [5, 20]$ UAVs with different

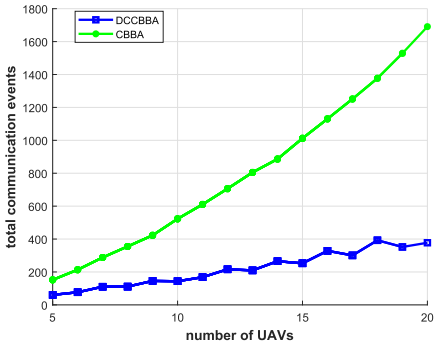

(a)

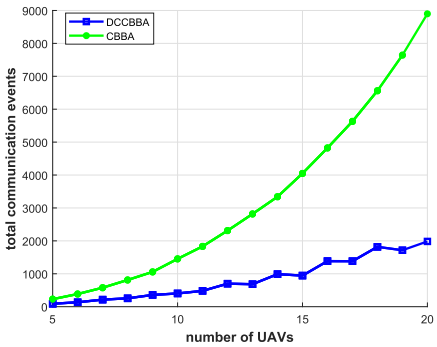

(b)

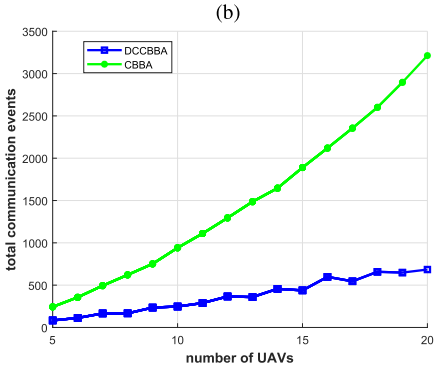

(c)

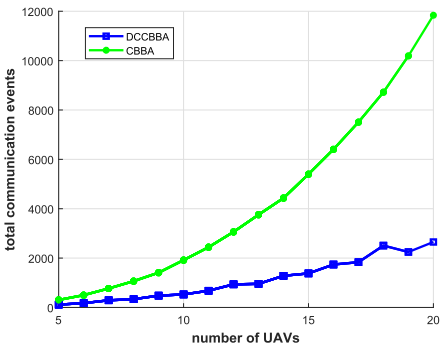

(d)

FIGURE 21. $N_a \in [5, 20]$ UAVs perform $N_T = 20$ reconnaissance tasks with different communication topologies. (a) Full, (b) Ring, (c) Star, (d) Chain.

communication topologies performing $N_T = 20$ reconnaissance tasks in this considered scenario. Other parameters of UAVs and tasks are the same as those in section VI-A and section VI-C. In addition, the baseline

CBBA is conducted to compare with DCCBBA to illustrate its efficiency. The performances of algorithms presented here are analyzed by running one hundred Monte-Carlo simulations. The mean performances of DCCBBA with different number of UAVs are presented in Fig. 21.

It can be seen that, with the increasing number of participating UAVs, an exponential rise in the total communication events required to keep the collective up to date is presented in baseline CBBA process while the total communication events of DCCBBA increase slightly as shown in Fig. 21, which results from that total communication events of baseline CBBA are exponential with N_a in equation (14) and total communication events of DCCBBA are linear with N_a in equation (15). In addition, compared with baseline CBBA, the number of communication events required to produce conflict-free assignments of DCCBBA is significantly lower, this is because that each UAV only needs to communicate with the vital communication node in the same cluster. Meanwhile, as the number of UAVs increases, the difference of communication events tends to be more significant when communication topology is a chain in Fig. 21(d). The reason is that more communication hops are required to obtain conflict-free assignments between UAVs.

VII. CONCLUSION

This paper presents a dynamic clustering consensus-based bundle algorithm, which improves bundle construction and consensus methods to bring parallelism to baseline CBBA to reduce the amount of communication in the conflict resolution phase. What is more, DCCBBA retains the robustness of distributed task allocation. Numerical simulations have been performed to illustrate the performance of DCCBBA under different scales of tasks, different communication topologies, different communication network density, different number of clusters and different number of UAVs. The simulation results have demonstrated the feasibility and reliability of DCCBBA compared with the baseline CBBA, CF-CBBA, GCBBA and Two-layer CBBA.

The framework presented in this paper suffers from some limitations. First, the DCCBBA is only guaranteed to converge in situations where all the bidding schemes satisfy the DMG property [7], as is the case for the baseline CBBA. Second, the locations of the tasks and UAVs are given at the beginning, further researches are required to improve the applicability of DCCBBA in dynamic and uncertain environment. In future work, methods of extending the application scenarios of the proposed DCCBBA and decreasing the computational complexity will form an element of future work to be undertaken. Furthermore, experimentations in both static and dynamic environments are considered to empirically validate the results presented in this paper.

ACKNOWLEDGMENT

The authors would like to thank the editors and reviewers for constructive comments.

REFERENCES

[1] H. Studiawan, G. Grispos, and K.-K.-R. Choo, "Unmanned aerial vehicle (UAV) forensics: The good, the bad, and the unaddressed," *Comput. Secur.*, vol. 132, Sep. 2023, Art. no. 103340.
[2] T. B. Shahi, C.-Y. Xu, A. Neupane, and W. Guo, "Recent advances in crop disease detection using UAV and deep learning techniques," *Remote Sens.*, vol. 15, no. 9, p. 2450, May 2023.
[3] S. Poudel and S. Moh, "Task assignment algorithms for unmanned aerial vehicle networks: A comprehensive survey," *Veh. Commun.*, vol. 35, Jun. 2022, Art. no. 100469.
[4] J. Tang, G. Liu, and Q. Pan, "A review on representative swarm intelligence algorithms for solving optimization problems: Applications and trends," *IEEE/CAA J. Autom. Sinica*, vol. 8, no. 10, pp. 1627–1643, Oct. 2021.
[5] J. C. Amorim, V. Alves, and E. P. de Freitas, "Assessing a swarm-GAP based solution for the task allocation problem in dynamic scenarios," *Expert Syst. Appl.*, vol. 152, Aug. 2020, Art. no. 113437.
[6] J. Tang, X. Chen, X. Zhu, and F. Zhu, "Dynamic reallocation model of multiple unmanned aerial vehicle tasks in emergent adjustment scenarios," *IEEE Trans. Aerosp. Electron. Syst.*, vol. 59, no. 2, pp. 1139–1155, Apr. 2023.
[7] H.-L. Choi, L. Brunet, and J. P. How, "Consensus-based decentralized auctions for robust task allocation," *IEEE Trans. Robot.*, vol. 25, no. 4, pp. 912–926, Aug. 2009.
[8] H.-L. Choi, A. K. Whitten, and J. P. How, "Decentralized task allocation for heterogeneous teams with cooperation constraints," in *Proc. Amer. Control Conf.*, Jul. 2010, pp. 3057–3062.
[9] G. P. Das, T. M. McGinnity, S. A. Coleman, and L. Behera, "A fast distributed auction and consensus process using parallel task allocation and execution," in *Proc. IEEE/RSJ Int. Conf. Intell. Robots Syst.*, San Francisco, CA, USA, Sep. 2011, pp. 4716–4721.
[10] F. Zitouni, S. Harous, and R. Maamri, "A distributed approach to the multi-robot task allocation problem using the consensus-based bundle algorithm and ant colony system," *IEEE Access*, vol. 8, pp. 27479–27494, 2020.
[11] L. Johnson, S. Ponda, H.-L. Choi, and J. How, "Improving the efficiency of a decentralized tasking algorithm for UAV teams with asynchronous communications," in *Proc. AIAA Guid., Navigat., Control Conf.*, 2010, p. 8421.
[12] R. Chen, J. Li, Y. Chen, and Y. Huang, "An agent-related asynchronous consensus method for fast scheduling of UAV swarm," in *Proc. Amer. Control Conf. (ACC)*, May 2023, pp. 490–496.
[13] X. Zheng, F. Zhang, T. Song, and D. Lin, "Heterogeneous multi-UAV distributed task allocation based on CBBA," in *Proc. IEEE Int. Conf. Unmanned Syst. (ICUS)*, Oct. 2019, pp. 704–709.
[14] W. Zhao, Q. Meng, and P. W. H. Chung, "A heuristic distributed task allocation method for multivehicle multitask problems and its application to search and rescue scenario," *IEEE Trans. Cybern.*, vol. 46, no. 4, pp. 902–915, Apr. 2016.
[15] M. Argyle, D. W. Casbeer, and R. Beard, "A multi-team extension of the consensus-based bundle algorithm," in *Proc. Amer. Control Conf.*, Jun. 2011, pp. 5376–5381.
[16] D. Smith, J. Wetherall, S. Woodhead, and A. Adekunle, "A cluster-based approach to consensus based distributed task allocation," in *Proc. 22nd Euromicro Int. Conf. Parallel, Distrib., Netw.-Based Process.*, Feb. 2014, pp. 428–431.
[17] X. Chen, P. Zhang, F. Li, and G. Du, "A cluster first strategy for distributed multi-robot task allocation problem with time constraints," in *Proc. WRC Symp. Adv. Robot. Autom. (WRC SARA)*, Aug. 2018, pp. 102–107.
[18] X. Fu, P. Feng, B. Li, and X. Gao, "A two-layer task assignment algorithm for UAV swarm based on feature weight clustering," *Int. J. Aerosp. Eng.*, vol. 2019, Nov. 2019, Art. no. 3504248.
[19] Y. Zhang, W. Feng, G. Shi, F. Jiang, M. Chowdhury, and S. H. Ling, "UAV swarm mission planning in dynamic environment using consensus-based bundle algorithm," *Sensors*, vol. 20, no. 8, p. 2307, Apr. 2020.
[20] K.-S. Kim, H.-Y. Kim, and H.-L. Choi, "A bid-based grouping method for communication-efficient decentralized multi-UAV task allocation," *Int. J. Aeronaut. Space Sci.*, vol. 21, no. 1, pp. 290–302, Mar. 2020.
[21] J. Chen, X. Qing, F. Ye, K. Xiao, K. You, and Q. Sun, "Consensus-based bundle algorithm with local replanning for heterogeneous multi-UAV system in the time-sensitive and dynamic environment," *J. Supercomput.*, vol. 78, no. 2, pp. 1712–1740, Feb. 2022.

[22] W. Wu, H. Lu, J. Xu, and Y. Sun, "Hierarchical optimization method of space patrol task assignment based on deep neural network and consensus-based bundle algorithm," *Acta Astronautica*, vol. 207, pp. 295–306, Jun. 2023.
[23] S. Raja, G. Habibi, and J. P. How, "Communication-aware consensus-based decentralized task allocation in communication constrained environments," *IEEE Access*, vol. 10, pp. 19753–19767, 2022.
[24] K.-S. Kim, H.-Y. Kim, and H.-L. Choi, "Minimizing communications in decentralized greedy task allocation," *J. Aerosp. Inf. Syst.*, vol. 16, no. 8, pp. 340–345, Aug. 2019.
[25] L. Brunet, H.-L. Choi, and J. How, "Consensus-based auction approaches for decentralized task assignment," in *Proc. AIAA Guid., Navigat. Control Conf. Exhib.*, 2008, p. 6839.
[26] O. Dorabiala, J. N. Kutz, and A. Y. Aravkin, "Robust trimmed k-means," *Pattern Recognit. Lett.*, vol. 161, pp. 9–16, Sep. 2022.
[27] Z. Xiyu, X. Ziyu, and W. Jinghua, "Research on task allocation of heterogeneous multi-robot based on cluster grouping algorithm," (in Chinese), *J. Aero Weaponry*, vol. 29, no. 4, pp. 100–109, 2022.
[28] A. Ullah, B. Wang, J. Sheng, J. Long, N. Khan, and Z. Sun, "Identifying vital nodes from local and global perspectives in complex networks?" *Expert Syst. Appl.*, vol. 186, Dec. 2021, Art. no. 115778.
[29] W. Maharani, Adiwijaya, and A. A. Gozali, "Degree centrality and eigenvector centrality in Twitter," in *Proc. 8th Int. Conf. Telecommun. Syst. Services Appl. (TSSA)*, Oct. 2014, pp. 1–5.
[30] M. Barthelemy, "Betweenness centrality in large complex networks," *Eur. Phys. J. B*, vol. 38, no. 2, pp. 163–168, 2004.
[31] K. Okamoto, W. Chen, and X.-Y. Li, "Ranking of closeness centrality for large-scale social networks," in *Frontiers in Algorithmics*. Berlin, Germany: Springer, 2008, pp. 186–195.
[32] B. Ruhnau, "Eigenvector-centrality—A node-centrality?" *Social Netw.*, vol. 22, no. 4, pp. 357–365, Oct. 2000.
[33] T.-H. Nguyen, H. Park, and L. Park, "Recent studies on deep reinforcement learning in RIS-UAV communication networks," in *Proc. Int. Conf. Artif. Intell. Inf. Commun. (ICAIIC)*, Feb. 2023, pp. 378–381.
[34] H. Bruyninckx and D. Reynaerts, "Path planning for mobile and hyper-redundant robots using Pythagorean hodograph curves," in *Proc. 8th Int. Conf. Adv. Robotics. Proceedings. ICAR*, Jul. 1997, pp. 595–600.
[35] T. Su, X. Liang, X. Zeng, and S. Liu, "Pythagorean-hodograph curves-based trajectory planning for pick-and-place operation of delta robot with prescribed pick and place heights," *Robotica*, vol. 41, no. 6, pp. 1651–1672, Jun. 2023.
[36] B. Kalkan, D. F. Scharler, H.-P. Schröcker, and Z. Šír, "Rational framing motions and spatial rational Pythagorean hodograph curves," *Comput. Aided Geometric Design*, vol. 99, Nov. 2022, Art. no. 102160.
[37] M. Shanmugavel, A. Tsourdos, R. Zbikowski, and B. White, "3D path planning for multiple UAVs using Pythagorean hodograph curves," in *Proc. AIAA Guid., Navigat. Control Conf. Exhibit*, Aug. 2007, p. 6455.
[38] A. M. Ikotun, A. E. Ezugwu, L. Abualigah, B. Abuhaija, and J. Heming, "K-means clustering algorithms: A comprehensive review, variants analysis, and advances in the era of big data," *Inf. Sci.*, vol. 622, pp. 178–210, Apr. 2023.
[39] F. Ye, J. Chen, Q. Sun, Y. Tian, and T. Jiang, "Decentralized task allocation for heterogeneous multi-UAV system with task coupling constraints," *J. Supercomput.*, vol. 77, no. 1, pp. 111–132, Jan. 2021.
[40] Z. Tuo, D. Hanqiang, G. Jialong, and H. Jian, "Dynamic target assignment of multiple unmanned aerial vehicles based on clustering of network nodes," *J. Syst. Simul.*, vol. 35, no. 4, p. 695, 2023.

SHAOKUN YAN received the B.S. degree in mechanical engineering and the M.S. degree in weapons system from Northwestern Polytechnical University, Xi'an, China, in 2015 and 2018, respectively. He is currently pursuing the Ph.D. degree with the School of Automation, Beijing Institute of Technology. His research interests include control and decision of unmanned systems.

YUANQING XIA (Senior Member, IEEE) was born in Anhui, China, in 1971. He received the M.S. degree in fundamental mathematics from Anhui University, Hefei, China, in 1998, and the Ph.D. degree in control theory and control engineering from the Beijing University of Aeronautics and Astronautics, Beijing, China, in 2001. From 2002 to 2003, he was a Postdoctoral Research Associate with the Institute of Systems Science, Academy of Mathematics and System Sciences, Chinese Academy of Sciences, Beijing. From 2003 to 2004, he was a Research Fellow with the National University of Singapore, Singapore, where he researched on variable structure control. From 2004 to 2006, he was a Research Fellow with the University of Glamorgan, Pontypridd, U.K. Since 2004, he has been an Associate Professor with the School of Automation, Beijing Institute of Technology, Beijing, where he has been a Professor since 2008. From 2007 to 2008, he was a Guest Professor with Innsbruck Medical University, Innsbruck, Austria. His current research interests include networked control systems, robust control and signal processing, and active disturbance rejection control.